



## Evaluation of OMPS/LP Stratospheric Aerosol Extinction Product Using SAGE III/ISS Observations

Zhong Chen<sup>1,2</sup>, Pawan K. Bhartia<sup>2</sup>, Omar Torres<sup>2</sup>, Glen Jaross<sup>2</sup>, Robert Loughman<sup>3</sup>, Matthew  
5 DeLand<sup>1</sup>, Peter Colarco<sup>2</sup>, Robert Damadeo<sup>4</sup> and Ghassan Taha<sup>5</sup>

<sup>1</sup>Science Systems and Applications, Inc., Lanham, MA, USA

<sup>2</sup>NASA Goddard Space Flight Center, Greenbelt, MA, USA

<sup>3</sup>Department of Atmospheric and Planetary Sciences, Hampton University, Hampton, VA, USA

10 <sup>4</sup>NASA Langley Research Center, Hampton, VA, USA

<sup>5</sup>GESTAR, Columbia, Maryland, USA

Correspondence to: Zhong Chen ([zhong.chen@ssaihq.com](mailto:zhong.chen@ssaihq.com))

### 15 Abstract

The Ozone Mapping and Profiler Suite Limb Profiler (OMPS/LP) has been flying on the  
Suomi NPP satellite since October 2011. It is designed to produce ozone and aerosol vertical  
profiles at 1.6 km vertical resolution over the entire sunlit globe. The Version 1.5 (V1.5) aerosol  
extinction retrieval algorithm provides aerosol extinction profiles using observed radiances at  
20 675 nm. The algorithm assumes Mie theory and a gamma function aerosol size distribution for  
the stratospheric aerosol that is derived from Community Aerosol and Radiation Model for  
Atmospheres (CARMA) calculated results and observations in April 2012. In this paper, we  
compare V1.5 LP aerosol profiles with SAGE III/ISS solar occultation observations for the  
period June 2017 – May 2019, when both measurements were available. Overall, LP extinction  
25 profiles agree with SAGE data to within  $\pm 25\%$  for the main aerosol layer between 19 and 27 km,  
even during periods perturbed by volcanic eruptions or intense forest fires. The slope parameter  
of linear fitting of LP extinctions with respect to SAGE measurements are close to 1.0, with  
Pearson's correlation coefficients of  $r \geq 0.95$ , indicating that the LP aerosol data are reliable in  
that altitude range. Comparisons of extinction time series show a high degree of correlation  
30 between LP and SAGE, indicating that the LP retrieved extinction variability in time is robust.  
On the other hand, we find that LP retrieved extinction is systematically higher than SAGE  
observations at altitudes above 28 km and systematically lower below 19 km in the tropics. This  
is likely due in part to the fact that the actual aerosol size distribution is altitude dependent, while  
the assumed size distribution in the V1.5 retrieval is assumed to be altitude independent and so it



may be less accurate for altitudes above 28 km and below 19 km where the size distribution is more variable. There are other reasons related to cloud contamination, wavelength limitations and the accuracy of both instruments at low aerosol loading.

## 5 1. Introduction

Knowledge of stratospheric aerosol optical depth and microphysical properties is important to accurately determine the magnitude of the radiative effect of aerosols, and thus their possible influence on climate (Ridley et al., 2014). The Ozone Mapping and Profiler Suite (OMPS) Limb Profiler (LP) is one of three OMPS instruments onboard the Suomi National  
10 Polar-orbiting Partnership (S-NPP) satellite (Flynn et al., 2007). S-NPP was launched in October 2011, into a sun-synchronous polar orbit with 13:30 local equator crossing time. The LP instrument collects limb scattered radiance data on a 2-D charge coupled device (CCD) array over a wide spectral range (290-1000 nm) and a wide vertical extent (0–80 km) through three parallel vertical slits. These spectra are primarily used to retrieve vertical profiles of ozone (Rault  
15 and Loughman, 2013; Kramarova et al., 2018), aerosol extinction coefficient (Loughman et al., 2018; Chen et al., 2018), and cloud-top height (Chen et al., 2016). The vertical sampling of LP measurements is about 1 km, and the vertical resolution of the retrieved profiles is approximately 1.6 km. More details about the OMPS/LP instrument design and capabilities are provided in Jaross et al. (2014).

20 Recently, a new aerosol size distribution (ASD) based on a gamma function was introduced in the version 1.5 algorithm (V1.5, Chen et al. 2018). Chen et al. (2018) tested the algorithm by comparing 7 months of data between OMPS/LP and the Stratospheric Aerosol and Gas Experiment III instrument onboard the International Space Station (SAGE III/ISS). The limited comparison showed the consistency of the aerosol extinction measurements from both  
25 instruments, with a correlation coefficient 0.97 and slope 1.05. Now that the version 1.5 OMPS/LP aerosol algorithm has become operational, and additional SAGE III/ISS data are available, we document here a comprehensive evaluation of this new version of the OMPS/LP aerosol product.

This work extends the previous results shown in Chen et al. (2018) to evaluate LP aerosol  
30 extinction profiles through comparison with independent data sets from SAGE III/ISS. The latest versions, i.e., version 1.5 of LP and version 5.1 of SAGE III/ISS, are used. The objective of this



comparison is to assess the reliability of the LP version 1.5 algorithm and to identify potential problems inherent due to the assumed ASD. The differences of aerosol extinctions observed by the two instruments are analyzed and discussed. The LP retrieval algorithm performance is re-evaluated and the impact of volcanic perturbations on the retrievals is investigated.

5

## 2. LP Algorithm Description

The previous version 1 aerosol retrieval algorithm for OMPS/LP is described in detail by Loughman et al. (2018). Here, we provide a brief description of key changes implemented in the retrieval algorithm for processing the V1.5 dataset.

10 In the V1.5 algorithm, a gamma function based ASD is assumed (Chen et al., 2018):

$$n(r) = \frac{dN}{dr} = \frac{N_0 \beta^\alpha r^{\alpha-1}}{\Gamma(\alpha)} \exp(-r\beta) \quad (1)$$

where  $n(r)$  is the number of particles  $N$  per unit volume with a size between radius  $r$  and  $r+dr$  ( $\text{cm}^{-3}\mu\text{m}^{-1}$ ),  $N_0$  is the total number density of aerosols ( $\text{cm}^{-3}$ ),  $\Gamma$  is Euler's gamma function,  $\alpha$  is the shape parameter and  $\beta$  ( $\mu\text{m}^{-1}$ ) is the scale parameter. At small radii this function follows a power law, while at large radii it follows an exponential function. The cross-section and aerosol scattering phase function are then calculated using Mie theory assuming liquid sulfate spherical particles with a refractive index from Russell et al. (1996). The  $\alpha$  and  $\beta$  parameters were determined by fitting the gamma distribution to size distributions for stratospheric sulfate simulated by the Community Aerosol and Radiation Model for Atmospheres (CARMA) module running online in the Goddard Earth Observing System (GEOS) global model (after English et al. 2011, Colarco et al. 2014). The fitted ASD yields an Angstrom Exponent (AE) of 2.08 and an effective radius ( $r_{\text{eff}}$ ) of  $0.18 \mu\text{m}$ , similar to the average values determined from SAGE II version 7.0 aerosol extinction data (Thomason et al., 2008; Damadeo et al., 2013) between 20 and 25 km (red and green dots in Figure 1), from measurements at 525 and 1020 nm taken during the period 2000-2005. This was a period when the stratosphere was relatively clean and roughly similar to the present day stratosphere. Note that average SAGE II AE values at 30 km (blue dots in Figure 1) are larger than a lower altitudes. The SAGE II observed variability of aerosol properties with altitude is related to variability in temperature and humidity fields that affects the aerosol size distribution and refractive index (Steele and Hamill, 1981), both of which have a direct effect on the aerosol scattering phase function. Assuming that the aerosol signal in

15  
20  
25  
30



line of sight radiances is proportional to the aerosol phase function, aerosol extinction profiles at 675 nm are retrieved using an iterative technique, based on Chahine's non-linear relaxation technique. Atmospheric pressure and temperature profiles used in this retrieval algorithm are obtained from the GEOS atmospheric analyses produced by NASA GSFC Global Modeling  
5 Assimilation Office (GMAO). For the LP aerosol product, retrievals are only performed for observations with solar zenith angle  $SZA < 88^\circ$ .

### 3. Evaluation Analysis

#### 3.1 SAGE III/ISS data

10 The SAGE III/ISS developed by the NASA Langley Research Center (LaRC) was launched to the International Space Station in February of 2017. SAGE III/ISS makes sunrise and sunset occultation measurements of aerosols and gas concentrations in the stratosphere and upper troposphere (Chu et al., 1998). The ISS travels in a Low-Earth orbit at an altitude of 330-435 km and at an inclination of  $51.6^\circ$ . With these orbital parameters, solar occultation  
15 measurement opportunities cover a large range of latitudes (between  $70^\circ\text{S}$  and  $70^\circ\text{N}$ ). The instrument measures up to 31 combined sunrise and sunset profiles each day. A general description of the solar occultation measurement technique is provided by McCormick et al. (1979). Aerosol extinction at nine wavelengths (384.2, 448.5, 520.5, 601.6, 676.0, 756.0, 869.2, 1021.2 and 1544.0 nm) are provided by SAGE III/ISS from the surface or cloud top to an  
20 altitude of 45 km, with a vertical resolution of 0.5 km at the tangent point location. The SAGE series of aerosol occultation measurements have been extensively evaluated and compared with other space based instruments and have been found to have relatively high precision and accuracy (Thomason et al., 2010, 2018; Bourassa et al., 2012; Kovilakam and Deshler, 2015; von Savigny et al., 2015; Rieger et al., 2018). In this work we use SAGE III/ISS version 5.1 data,  
25 including both sunrise and sunsets, which were collected during the period June 2017 – May 2019. Figure 2 shows the spatial and temporal coverage of the available datasets during the 2017 to 2019 period considered in this study.

#### 3.2 Methodology

30 Chen et al. (2018) described previous LP-SAGE III/ISS comparisons using SAGE III/ISS version 5.0 data for the period of seven months from June to December of 2017. The first comparison was conducted in two steps. First, all data were binned and averaged in  $10^\circ$  latitude



bins for each altitude for groups of 1-3 consecutive days depending on the number of SAGE samples. In the second step, the averaged extinction profiles at 675 nm for LP and at 676 nm for SAGE were compared directly, using SAGE samples that correspond to the OMPS/LP 1 km altitude grid.

5 In this work, both data sets were averaged zonally for each 5° latitude band per day at each of their respective altitudes. The daily averaged data in the same latitude bin and on the same day were used for the comparison. Only LP data from the center slit were taken into consideration because the center slit has better straylight and tangent height corrections compared to the left and right slits (Moy et al., 2017; Kramarova et al., 2018), and all LP data  
10 below the OMPS/LP reported cloud height were rejected.

As SAGE science team pointed out (Thomason, L., personal communication; Thomason and Taha, 2003), reported SAGE III/ISS aerosol extinction is retrieved as a residual using a spectrally-focused fitting (i.e., it derives from the “MLR” ozone product) and any bias in ozone would result in a bias in the aerosol extinctions in the vicinity of the Chapuis band depending  
15 upon altitude and ozone concentration. To avoid possible biases in the SAGE III/ISS reported 676 nm aerosol extinction, associated with remaining ozone absorption effects, the aerosol channels at 449 nm and 756 nm were used in this study to interpolate to 675 nm SAGE extinction profiles. Figure 3a shows SAGE III/ISS profiles of reported (black line), and  
20 recalculated by interpolation (green line) 675 nm aerosol extinction at 0.5 km vertical resolution. Large differences between reported and recalculated SAGE extinctions values are apparent above 27 km. The extinction minimum at 29 km in the original data is not present in the interpolated profile. Also shown is the corresponding LP profile (blue line) at 1.0 km sampling grid. Since the SAGE data are given at 0.5 km intervals, while the vertical resolution of LP is around 1.6 km, the vertical resolution of SAGE was then degraded to match the OMPS vertical  
25 resolution using a 7-point binomial smoothing function given by the expression:

$$k(z) = \sum_{i=-1}^7 k(z + \Delta z_i) * w(i),$$

$$\Delta z_i = -1.5, -1, -0.5, 0.0, 0.5, 1, 1.5, \text{ and } w(i) = [1, 6, 15, 20, 15, 6, 1]/64 \quad (2)$$

where  $k$  is the extinction,  $w$  is the weighing factor and  $z$  is the altitude grid point. This procedure approximates a Gaussian smoothing of continuous data with full width at half maximum of about  
30 1.6 km. Figure 3b provides an example of comparison of extinction profiles between the LP retrieval profile (blue line) and the smoothed version of the recalculated SAGE profiles (red



line). LP data is in close agreement with the SAGE record between 20 and 30 km. This spectrally interpolated and vertically smoothed SAGE data is used for all comparisons in this paper.

## 4. Results and discussion

### 5 4.1 Background aerosol conditions

Figure 4 depicts time series of OMPS/LP (blue symbols) and SAGE III/ISS (red symbols) at 20.5 km, 25.5 km and 30.5 km in the tropics from June 2017 through May 2019. The time dependent variability of each dataset is similar and data features associated with specific aerosol events observed by SAGE are also present in the LP record. The observed large aerosol extinction increase at 20 km apparent in both data records by the end of 2018, is associated with the eruption of Mt. Ambae (June 2018 at 15°S). At 20.5 km and 25.5km, LP and SAGE are within 20% of each other, indicating that the assumed ASD in LP v1.5 algorithm is reasonable. The large temporal variability present in both datasets at 30.5 km is probably related to Quasi-Biennial Oscillation (QBO) effects (Plumb and Bell, 1982; Thomason et al., 2008). At 30.5 km, the agreement is not quite as good. At this altitude, LP retrievals are still higher than SAGE extinctions for all latitude bins. The systematic positive bias between LP and SAGE may be due to the fact that the actual ASD, and refractive index, which depend on temperature and humidity (Steele and Hamill, 1981), are not truly independent of height as currently assumed in the LP algorithm (see Figure 11).

The time series of aerosol extinction from OMPS/LP and SAGE III/ISS measurements at northern and southern mid-latitudes are compared in Figure 5. The results are very similar to comparisons in the tropics (Figure 4), showing that the aerosol extinctions are highly variable in altitude and time. LP shows a negative bias at 20.5km in the southern mid-latitudes, as well as seasonal variations that are not seen by SAGE, mostly caused by ASD errors and limitation of 675 when observing in backscatter condition. Canadian pyro-cumulonimbus (PyroCb) was responsible for increasing aerosol extinctions at 20.5 km in latitude bin 30°N-35°N (left column) in late 2017. The LP-SAGE comparisons show generally good agreement between the two data sets, but poorer agreement up to about a factor of 4 for the 30.5 km altitude over polar regions (near 55°S and 60°N), where the aerosol concentrations are very low. Under low aerosol condition, both instruments are less sensitive to smaller aerosols. For SAGE, the AE is quite scattered at 30 km compared to lower altitude (see Figure 1), which is related to reduced quality



of the aerosol retrieval for low aerosol values, while straylight contamination is more obvious at 30 km for OMPS/LP.

#### 4.2 Effect of volcanic eruptions and PyroCb's

5 To investigate the impacts of volcanic eruptions and intense wildfires on the LP retrievals, aerosol extinction profiles from OMPS/LP and SAGE III/ISS were inter-compared in the aftermath of the eruption of Mt. Ambae (2018) and the Canadian wildfires (2017) sampled by these instruments. The daily averaged data in the same latitude bin and on the same day were used for the comparison.

10 Volcanic eruptions are the largest source of long-lived aerosols in the stratosphere. The Ambae eruption occurred on July 27, 2018, in Ambae Island located near 15° S, 167°E and had a clear impact on the stratospheric aerosol load. Top panel of Figure 6 shows comparisons of LP and SAGE zonally averaged stratospheric aerosol profiles between 0–5°N on three days before the eruption (first three plots), along with the relative differences on each day (fourth plot). Pre-  
15 eruption LP measurements agree within 5% of SAGE observations over the 20-25 km altitude range. Larger differences (up to 20%) are observed for post-eruption conditions as shown on a similar set of plots shown on the bottom panel of Figure 6. The enhanced extinction around 20 km after the eruption was captured by both OMPS/LP and SAGE III/ISS observations. Much larger differences between the two data sets are apparent below 20 km and above 25 km both  
20 before and after the volcanic eruption.

In addition to volcanic eruptions, intense wildfires can also cause aerosol perturbations in the upper troposphere and lower stratosphere (UTLS). On August 12, 2017, PyroCb storms from intense wildfire were produced in British Columbia, Canada (Peterson et al., 2018; Torres et al. 2019, submitted to JGR). A before-and-after analysis, similar to the one above for volcanic  
25 eruptions, was carried out to evaluate the performance of the LP algorithm following the stratospheric injection of carbonaceous aerosols. Zonal averages of SAGE and LP aerosol extinction retrievals for the 45°N–50°N latitude belt before and after the aerosol injection effect were compared (Figure 7). Both instruments clearly captured the stratospheric aerosol perturbation triggered by the reported PyroCb, including the elevation in the plume altitude over  
30 time. As in the previous analysis, the pre-injection level of agreement between the two data sets is better than 5% between 20 km and 25 km, whereas slightly larger differences (~10%) in the



same altitude range are found several days following the arrival in the stratosphere of the carbonaceous aerosols. Unrelated to this event, SAGE-LP discrepancies below 20 km and above 25 km are significantly larger.

#### 5 4.3 LP retrievals above 27 km and below 19 km

All comparisons shown in Figures 4–7 have some features in common. The best agreement is found for the main aerosol layer range roughly between 19 and 27 km, but systematic and significant differences are observed above 28 km and below 19 km. These systematic differences change with altitude and may be associated with the algorithm assumption of time and altitude independent aerosol model (i.e., refractive index and ASD) and the corresponding aerosol scattering phase function (PF). SAGE can't measure the PF but the aerosol spectrum (in this case the approximation of the AE) can be used as an effective qualitative indicator of particle size (Hayashida et al., 2001; Schuster et al., 2006; Damadeo et al., 2013; Rieger et al., 2018).

To examine the LP algorithm performance of the aerosol retrieval due to the assumed ASD, we perturbed the nominal gamma ASD fitting parameters so that the resulting AE yielded values of 2.3 and 1.8 (about  $\pm 10\%$  of the algorithm's baseline value of 2.08). The 2.3 value is close to the reported average SAGE II AE at 30 km for the period 2000-2005 (blue dots in Figure 1) whereas the AE value of 1.8 resembles similar SAGE II average at 18 km. The perturbed ASD's, associated with AE values of 1.8 and 2.3, were used to estimate the resulting effect on the calculated 675 nm PF as shown in Figure 8. A  $\pm 10\%$  change in AE can produce a about  $\pm 15\%$  change in PF. The results of the sensitivity analysis in Figure 8, indicates that changes in assumed PF will result in significant changes in retrieved aerosol extinctions.

Figure 9 shows that the use of the baseline AE value (2.08) produces significant error (up to  $\pm 13\%$ ) in retrieved extinction at 30.5 km and 18.5 km relative to the outcome when using AE values comparable to those from SAGE II v7.0 data. The results of this sensitivity analysis show that when taking into account the vertical variability of stratospheric aerosol properties, the LP algorithm performance improves at all levels. Figure 10 shows differences in aerosol extinction between OMPS/LP and SAGE III/ISS at 30.5 km in the tropics (top) and at 18.5 km in northern middle latitudes (bottom) plotted as a function of LP scattering angle for the entire comparison period to see if an ASD error exists. As discussed earlier, if the assumed ASD is correct, the





5 difference in extinction should be scattering angle independent in the scattering angle range 50°–100°. The differences shown in Figure 10 vary with scattering angle in that range significantly, suggesting the currently assumed ASD in the LP algorithm does not adequately represent the actual ASD for altitudes at 30.5 km and 18.5 km. As a result, the potential ASD error propagates into extinction uncertainties above 28 km and below 19 km.

#### 4.4 Correlation of the extinction and the Angstrom exponent

10 The sensitivities given in Figures 8-10 suggest that the differences in extinctions between the two instruments could be partly explained with the variation of the AE Figure 11 illustrates how the AE varies. In the figure, monthly mean AE (left panel) derived from vertically smoothed SAGE III/ISS data and differences between SAGE III/ISS and OMPS/LP extinctions at 675 nm (right panel) are plotted as a function of altitude and time at different latitude bands in the tropics. To draw a corollary to SAGE II, the AE is derived using the aerosol extinctions at 520nm and 1020nm. However, to avoid potential bias, the aerosol extinction is first interpolated  
15 using a second order polynomial in log-log space (extinction versus wavelength) with extinction values at 448nm, 756nm, 869nm, and 1020nm. The computed AE is plotted on a color scale with the baseline value of 2.08 used for the OMPS-LP algorithm at its center. AE values above the baseline are easily associated with the volcanic eruption of Mt. Ambae (note transport from the QBO) and aerosol evaporation at higher altitudes (particularly in the tropics). AE values  
20 below the baseline are easily associated with clouds (and a minor influence from the PyroCb). There also appears to be an overall bias towards an AE value slightly below the baseline throughout most of the stratosphere. The figure also shows a clear correlation between the difference between assumed AE and AE derived by SAGE and the difference between the instruments in the tropical stratosphere, which confirms that the altitude independent ASD is a  
25 cause for these systematic biases. However, there is an expectation of differences at the southern midlatitudes where the relationship between AE and PF at a given scattering angle is more complicated due to a competing effect from aerosol scattering and Rayleigh attenuation.

#### 4.5 Regression analysis

30 Figure 12 shows scatter plots of individual daily zonal mean extinction values from OMPS/LP and SAGE III/ISS for 5° latitude bands for 60° S -30° S (left panel), 30° S - 30° N



(middle panel) and 30° N - 60° N (right panel). The corresponding comparison statistics are written within the plot. While the overall impression from these results is encouraging, the agreement changes with latitude. In the tropics and northern midlatitudes (30° S - 30° N and 30° N - 60° N), there is a good agreement between the results from both instruments, with most observations close to the 1:1 line and a correlation coefficient greater than 0.96. This result gives further quantitative evidence that the assumed ASD is appropriate for OMPS/LP aerosol extinction retrievals in most of the stratosphere for background aerosol. In the southern midlatitudes between 60° S -30° S, zonal means from LP and SAGE are in fair agreement with a correlation coefficient of 0.95, but large systematic differences (SAGE III greater than LP) are observed for aerosol extinction,  $k > 0.0001$ . These positive deviations up to 25% could be related to wavelength limitations. Figure 13 shows an example of aerosol weighting functions at 675 nm for three latitudes. In general, the sensitivity to aerosol varies with latitude and altitude. The LP radiance at 675 nm is most sensitive to the aerosol extinction over the 20-30 km altitude range in the tropics and the northern midlatitudes, but less sensitive to aerosol in the southern midlatitudes. Therefore, uncertainties in OMPS/LP aerosol retrievals at 675 nm increase with reduced sensitivity to aerosol extinction because lower sensitivities to aerosol may result in noise amplification. Since the sensitivity to aerosol increases at longer wavelengths (Taha et al., 2011), the uncertainties in the southern midlatitudes at lower altitude may be reduced by doing LP aerosol retrieval at longer wavelengths.

20

## 5. Summary and Conclusions

To extend our previous validation of OMPS/LP aerosol product, OMPS/LP version 1.5 extinction profiles have been compared against SAGE III/ISS version 5.1 aerosol data over the period June 2017 to May 2019. For the comparison, both LP and SAGE extinction profiles in this paper are in the form of daily averages for a 5° latitude bin at each altitude. To evaluate the 675 nm extinction profilers from OMPS/LP, the original SAGE extinctions at 449 nm and 756 nm are used to interpolate to the extinction profiles at 675 nm, to avoid contamination from potential biases in the SAGE “MLR” ozone product, and then degraded vertically to the same 1.6 km vertical resolution as OMPS/LP. Using SAGE aerosol channels away from the Chappius and matching the vertical resolution of the instruments significantly improves the comparisons.

30



Overall, results show very good agreement for extinction profiles in the main aerosol layer between 19 to 27 km, to within  $\pm 25\%$ , and show systematic differences (LP-SAGE) above 28 km and below 19 km ( $> \pm 25\%$ ). The agreement changes with time, altitude and latitude. Comparisons of time series show strong correlation between the two data sets, indicating that measured extinction variability is robust. To investigate the impacts of volcanic perturbations on the retrievals, the differences of extinction profiles measured by LP and SAGE III/ISS in the same latitude bin and on the same day are analyzed before and after the occurrence of the Mt. Ambae volcanic eruption and the Canadian PyroCb. The results show that both instruments can capture the volcanic aerosol and PyroCb very well, and their small discrepancies ( $< \pm 10\%$ ) are within the measurement uncertainties, indicating that the LP retrieved extinction profiles are reliable under these conditions. In order to better quantify the difference in the variability observed in the OMPS/LP and SAGE III/ISS measurements, a total of 9862 data points between 19.5 km and 27.5 km were used to perform a linear regression analysis. The regression results show very high correlations with the linear correlation coefficient greater than 0.95, and most observations lie close to the 1:1 line, except for the southern midlatitudes where large positive differences up to 25% are observed due to differences in retrieval techniques and sensitivity issue. These comparisons are consistent with the previous analysis performed by Chen et al. (2018) that demonstrated a good agreement between the extinction profiles in the range of 19 to 29 km, differing above 30 km and below 19 km.

At altitudes above 28 km (below 19 km), LP extinctions were systematically higher (lower) than SAGE observations. These significant and systematic biases between LP and SAGE are partly due to the fact that the actual ASD is both altitude and time dependent. To evaluate the LP performance of the aerosol retrieval from the assumed ASD, the averaged Angstrom exponent (AE) derived from SAGE II v7.0 data under background aerosol conditions was compared with the baseline AE derived from the assumed ASD. The analysis indicates that in background conditions, the baseline AE is underestimated (overestimated) above 28 km (below 19 km), thus the assumed ASD provides a less accurate representation at altitudes above 28 km (below 19 km), tending to overestimate (underestimate) extinctions above 28 km (below 19 km). This suggests that a dynamic model for ASD is needed to accurately retrieve aerosol extinction profiles.



There are three other possible causes for the discrepancies. First, most of the discrepancies are related to differences in the measurement techniques. While SAGE III/ISS uses the solar occultation measuring technique which is self-calibrating and derives extinction directly, OMPS/LP employs the limb scatter technique where retrieved extinction depends on instrument calibration and altitude registration as well as the inversion algorithm and its several assumptions, especially the dependence of the OMPS retrieval on the assumed ASD and phase function. Uncertainties in OMPS/LP aerosol retrievals at 675 nm increase below 18 km due to lower sensitivities to aerosol. Second, some discrepancies could be also caused by reduced aerosol loading and hence reduced retrieval accuracy for both instruments. For OMPS, straylight contamination is more obvious under low aerosol conditions, where SAGE III quality decreases. Third, a larger random discrepancy between LP and SAGE at lower altitudes is associated with broken clouds at various locations and levels. The cloud contamination can affect extinction profiles near and below the tropopause. OMPS/LP version 1.5 aerosol profiles are freely available to the international research community at <https://disc.gdfc.nasa.gov>.

15

### Acknowledgements

We thank the OMPS/LP team at NASA Goddard and Science Systems and Applications, Inc. (SSAI) for help in producing the data used in this study. We also would like to thank Philippe Xu and Tong Zhu for their technical support.

20

### References

- Bourassa, A., Rieger, L., Lloyd, D., and Degenstein, D.: Odin-OSIRIS stratospheric aerosol data product and SAGE III intercomparison, *Atmos. Chem. Phys.*, 12, 605–614, 2012.
- Chen, Z., DeLand, M., and Bhartia, P. K.: A new algorithm for detecting cloud height using OMPS/LP measurements, *Atmos. Meas. Tech.*, 9, 1239–1246, doi:10.5194/amt-9-1239-2016, 2016.
- Chen, Z., Bhartia, P. K., Loughman, R., Colarco, P. and DeLand, M.: Improvement of stratospheric aerosol extinction retrieval from OMPS/LP using a new aerosol model, *Atmos. Meas. Tech.*, 11, 6495–6509, 2018 <https://doi.org/10.5194/amt-11-6495-2018>, 2018.
- Chu, W., and Veiga, R.: SAGE III/EOS, *Proc. SPIE 3501, Optical Remote Sensing of the Atmosphere and Clouds*, 52–60, doi:10.1117/12.577943, August 1998.
- Colarco, P. R., Nowottnick, E. P., Randles, C. A., Yi, B., Yang, P., Kim, K.-M., Smith, J. A., and Bardeen, C. G.: Impact of radiatively interactive dust aerosols in the NASA GEOS-5 climate model: Sensitivity to dust particle shape and refractive index, *J. Geophys. Res. Atmos.*, 119, 753–786, doi:10.1002/2013JD020046, 2014.

35



- Damadeo, R. P., Zawodny, J. M., Thomason, L.W., and Iyer, N.: SAGE version 7.0 algorithm: application to SAGE II, *Atmos. Meas. Tech.*, 6, 3539–3561, 2013.
- English, J. M., Toon, O. B., Mills, M. J., and Yu, F.: Microphysical simulations of new particle formation in the upper troposphere and lower stratosphere, *Atmos. Chem. Phys.*, 11, 9303–9322, doi:10.5194/acp-11-9303-2011, 2011, [www.atmos-chem-phys.net/11/9303/2011](http://www.atmos-chem-phys.net/11/9303/2011)
- 5 Flynn, L. E., Seftor, C. J., Larsen, J. C., and Xu, P.: The Ozone Mapping and Profiler Suite, in: *Earth Science Satellite Remote Sensing*, edited by: Qu, J. J., Gao, W., Kafatos, M., Murphy, R. E., and Salomonson, V. V., Springer, Berlin, 279–296, doi:10.1007/978-3-540-37293-6, 2007.
- 10 Hayashida, S., Horikawa, M., Anti-Correlation between stratospheric aerosol extinction and the Ångström parameter from multiple wavelength measurements with SAGE II—A characteristic of the decay period following major volcanic eruptions, *Geophys. Res. Lett.*, 28, 4063–4066, 2001, doi:10.1029/2000GL012826, 2001.
- Jaross, G., Bhartia, P. K., Chen, G., Kowitt, M., Haken, M., Chen, Z., Xu, P., Warner, J.,  
15 and Kelly, T.: OMPS Limb Profiler instrument performance assessment, *J. Geophys. Res. Atmos.*, 119, 4399–4412, doi:10.1002/2013JD020482, 2014.
- Kovilakam, M. and Deshler, T.: On the accuracy of stratospheric aerosol extinction derived from in situ size distribution measurements and surface area density derived from remote SAGE II and HALOE extinction measurements, *J. Geophys. Res. Atmos.*, 120, 8426–8447,  
20 doi:10.1002/2015JD023303, 2015.
- Kramarova, N. A., Bhartia, P. K., Jaross, G., Moy, L., Xu, P., Chen, Z., DeLand, M., Froidevaux, L., Livesey, N., Degenstein, D., Bourassa, A., Walker, K. A., and Sheese, P.: Validation of ozone profile retrievals derived from the OMPS LP version 2.5 algorithm against correlative satellite measurements, *Atmos. Meas. Tech.*, 11, 2837–2861, doi:10.5194/amt-11-2837-2018, 2018.
- 25 Loughman, R., Bhartia, P. K., Chen, Z., Xu, P., Nyaku, E., and Taha, G.: The Ozone Mapping and Profiler Suite (OMPS) Limb Profiler (LP) Version 1 aerosol extinction retrieval algorithm: theoretical basis, *Atmos. Meas. Tech.*, 11, 2633–2651, doi:10.5194/amt-11-2633-2018, 2018.
- 30 McCormick, M. P., Hamill, P., Pepin, T. J., Chu, W. P., Swissler, T. J., and McMaster, L. R.: Satellite studies of the stratospheric aerosol, *Bull. Amer. Meteor. Soc.*, 60, 1038, 1979.
- Moy, L., Bhartia, P. K., Jaross, G., Loughman, R., Kramarova, N., Chen, Z., Taha, G., Chen, G., and Xu, P.: Altitude registration of limb-scattered radiation, *Atmos. Meas. Tech.*, 10, 167–178, doi:10.5194/amt-10-167-2017, 2017.
- 35 Plumb, R. A., and R. C. Bell, A model of the quasi-biennial oscillation on an equatorial beta-plane. *Quart. J. Roy. Meteor. Soc.*, 108, 335–352, 1982.
- Peterson, D. A., Campbell, J. R., Hyer, E. J., Fromm, M. D., Kablick, G. P., Cossuth, J. H., & DeLand, M. T., Wildfire-driven thunderstorms cause a volcano-like stratospheric injection of smoke. *Npj Climate and Atmospheric Science*, <https://doi.org/10.1038/s41612-018-0039-3>,  
40 2018.



- Rault, D. F., and Loughman, R. P.: The OMPS Limb Profiler Environmental Data Record algorithm theoretical basis document and expected performance, *IEEE Trans. Geosci. Remote Sens.*, 51(5), 2505–2527, 2013.
- Ridley, D. A., Solomon, S., Barnes, J. E., Burlakov, V. D., Deshler, T., Dolgii, S. I., Herber, A. B., Nagai, T., Neely III, R. R., Nevzorov, A. V., Ritter, C., Sakai, T., Santer, B. D., Sato, M., Schmidt, A., Uchino, O., and Vernier, J. P.: Total volcanic stratospheric aerosol optical depths and implications for global climate change, *Geophys. Res. Lett.*, 41, 7763–7769, doi:10.1002/2014GL061541, 2014.
- Rieger, L. A., Malinina, E. P., Rozanov, A. V., Burrows, J. P., Bourassa, A. E., and Degenstein, D. A.: A study of the approaches used to retrieve aerosol extinction, as applied to limb observations made by OSIRIS and SCIAMACHY, *Atmos. Meas. Tech.*, 11, 3433–3445, doi:10.5194/amt-11-3433-2018, 2018.
- Russell, P.B. et al., Global to microscale evolution of the Pinatubo volcanic aerosol, derived from diverse measurements and analyses, *J. Geophys. Res.*, 101, 18745–18763, 1996.
- Schuster, G. L., Dubovik, O., Holben, B.N., Angstrom exponent and bimodal aerosol size distributions, *J. Geophys. Res. Atmos.*, 111, D07207, 2006, doi:10.1029/2005JD006328, 2006.
- Steele H. and P. Hamill, Effects of temperature and humidity on the growth and optical properties of sulphuric acid-water droplets in the stratosphere, *J. Aerosol Sci.*, 12(6), 517–528, 1981.
- Taha, G., Rault, D. F., Loughman, R. P., Bourassa, A. E. and von Savigny, C.: SCIAMACHY stratospheric aerosol extinction profile retrieval using the OMPS/LP algorithm, *Atmos. Meas. Tech.*, 4, 547–556, 2011, doi:10.5194/amt-4-547-2011
- Thomason, L. W. and Taha, G.: SAGE III aerosol extinction measurements: Initial results, *Geophys. Res. Lett.*, 30, NO. 12, 1631, doi:10.1029/2003GL017317, 2003.
- Thomason, L. W., Burton, S. P., Luo, B.-P., and Peter, T.: SAGE II measurements of stratospheric aerosol properties at non-volcanic levels, *Atmos. Chem. Phys.*, 8, 983–995, doi:10.5194/acp-8-983-2008, 2008.
- Thomason, L. W., Moore, J. R., Pitts, M. C., Zawodny, J. M., and Chiou, E.W.: An evaluation of the SAGE III version 4 aerosol extinction coefficient and water vapor data products, *Atmos. Chem. Phys.*, 10, 2159–2173, doi:10.5194/acp-10-2159-2010, 2010.
- Thomason, L. W., Ernest, N., Millán, L., Rieger, L., Bourassa, A., Vernier, J.-P., Manney, G., Luo, B., Arfeuille, F., and Peter, T.: A global space-based stratospheric aerosol climatology: 1979–2016, *Earth Syst. Sci. Data*, 10, 469–492, <https://doi.org/10.5194/essd-10-469-2018>, 2018.
- von Savigny, C., Ernst, F., Rozanov, A., Hommel, R., Eichmann, K.-U., Rozanov, V., Burrows, J. P., and Thomason, L. W.: Improved stratospheric aerosol extinction profiles from SCIAMACHY: validation and sample results, *Atmos. Meas. Tech.*, 8, 5223–5235, doi:10.5194/amt-8-5223-2015, 2015.



5

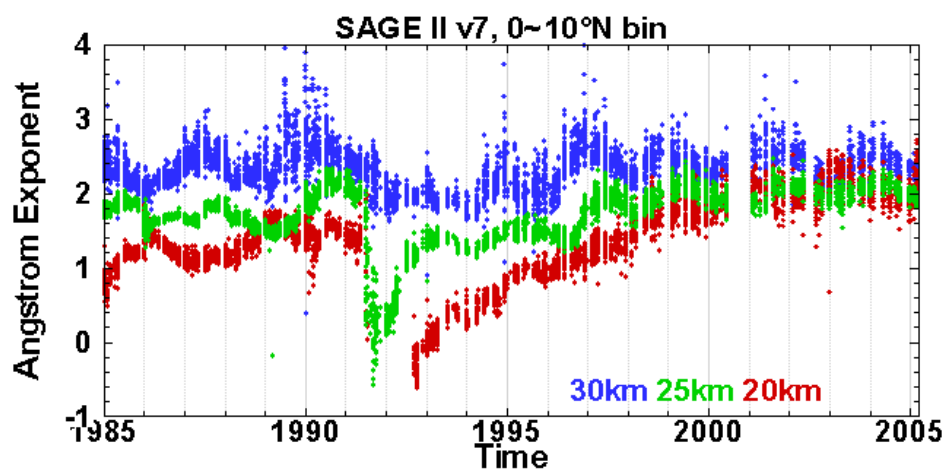


**Figure 1.** Time series of Angstrom Exponent (AE) derived from the aerosol extinction coefficient at 525 nm and 1020 nm for altitude at 30 km (blue), 25 km (green) and 20 km (red). This figure shows SAGE II version 7.0 data for the 0–10° N latitude band during the period 1986 - 2005. While the Pinatubo eruption in 1991 produced a significant decrease in AE, the smaller volcanic eruptions such as Ruang/Reventador in 2002 and Manam in 2005, visible in the extinction time series (not shown), did not appreciably affect AE values. The AE values appear to stabilize after 2000, suggesting that a background state exists. The AE is quite scattered at 30km compared to lower altitude, which is related to reduced quality of the aerosol retrieval for low aerosol values.

20

25

30



5

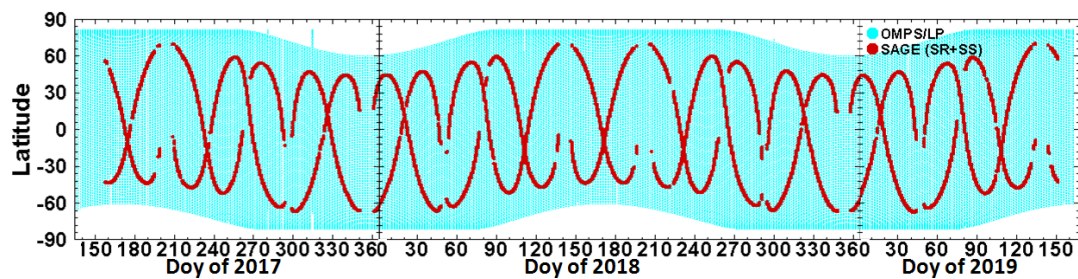


**Figure 2.** Time-latitude sampling pattern for OMPS/LP (light blue) and SAGE III/ISS (red) during the period of June 2017 – May 2019.

10

15

20

25

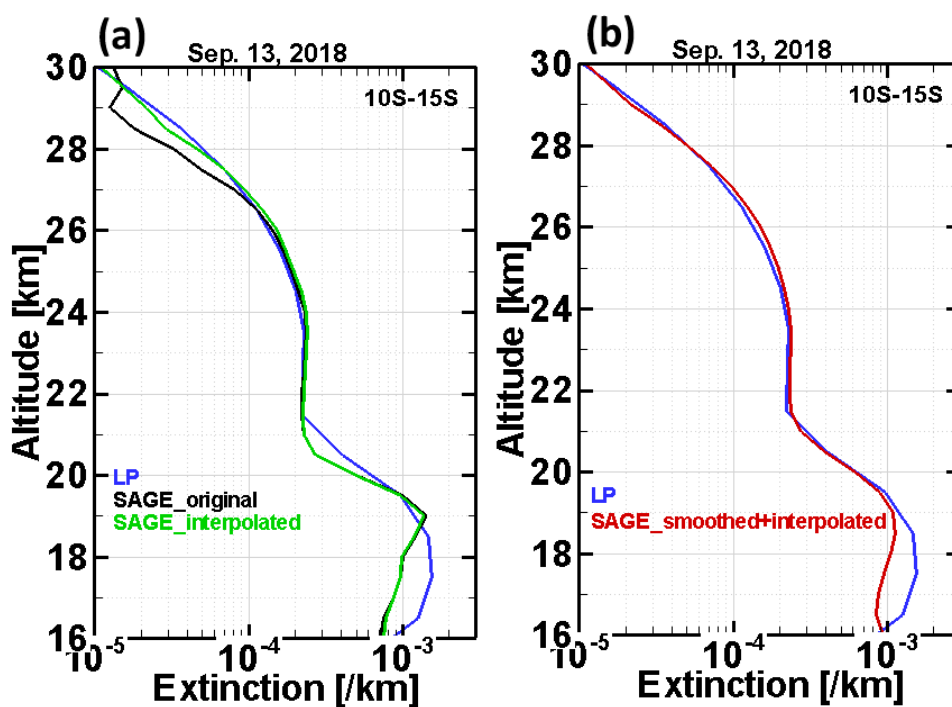
30

35





5



10 **Figure 3.** An example of LP-SAGE comparison of average extinction profiles in latitude bin 10–15°S for  
one day on September 13, 2018. **(a)** Comparison of extinction profiles among original SAGE (black),  
interpolated SAGE (green) and retrieved LP (blue). **(b)** Comparison of extinction profiles between the  
smoothed version of the recalculated SAGE profile (red) and the LP retrieval profile. Applying a  
combination of the smoothing and interpolation approaches to the original SAGE data improves the  
15 comparison above 27 km and below 21 km.

20



5

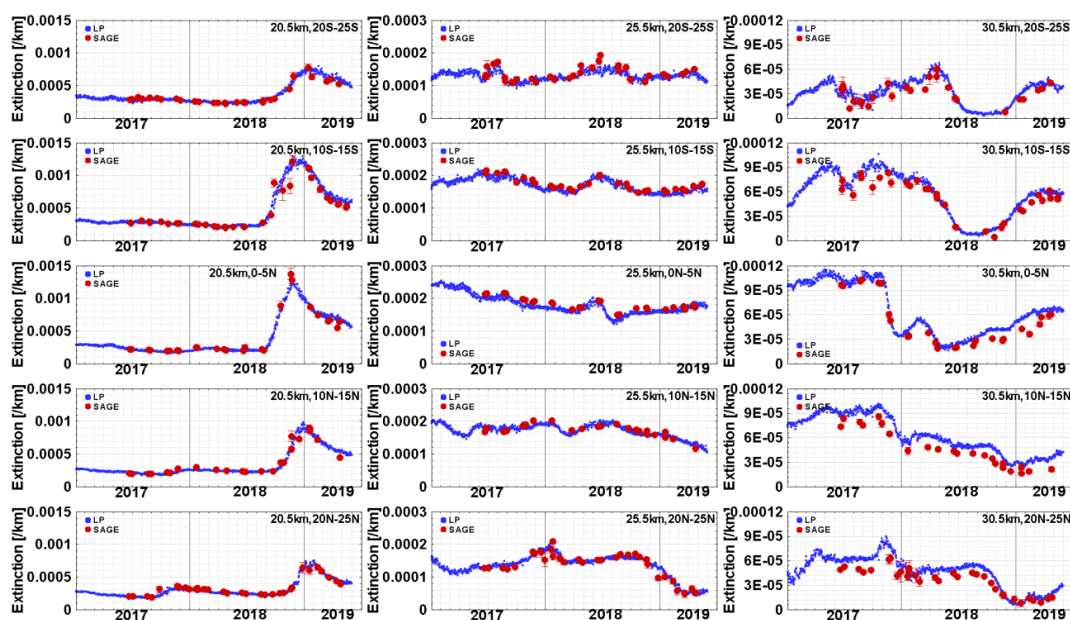


**Figure 4.** Comparison of the daily zonal mean time series of LP v1.5 (blue) and SAGE III/ISS v5.1 (red) extinctions at 675 nm for altitude at 20.5km (left), 25.5km (middle column) and 30.5km (right) for 5 degree latitude bands in the tropics (20°S–25°S, 10°S–15°S, 0°–5°N, 10°N–15°N, and 20°N–25°N, from the top to bottom) during the period June 2017 – May 2019. Vertical error bars on the SAGE measurements indicate standard error of the mean,  $\sigma/\sqrt{N}$ .

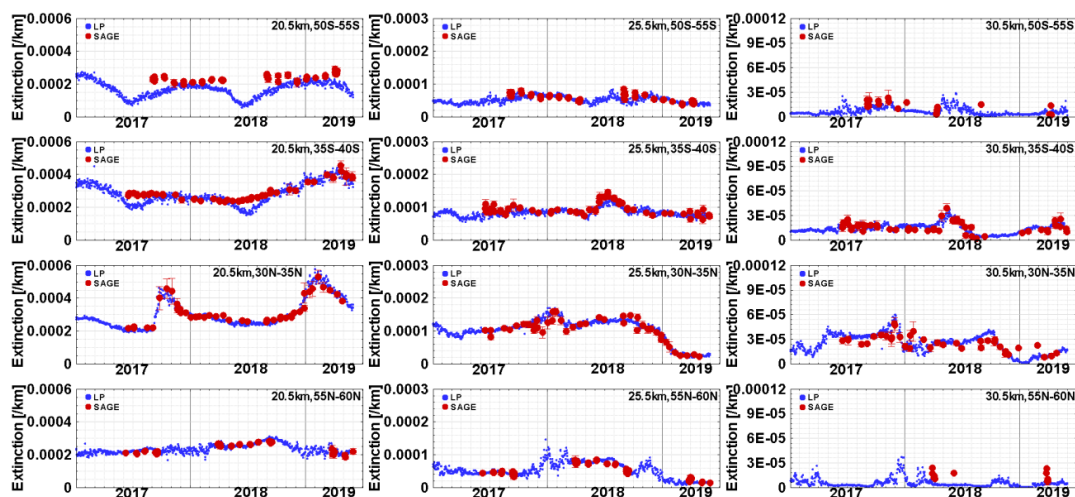
10

15

20



5



10 **Figure 5.** Same as Figure 4, but for latitude bands in 50°S–55°S, 35°S–40°S, 30°N–35°N, and 55°N–60°N (from the top to bottom).

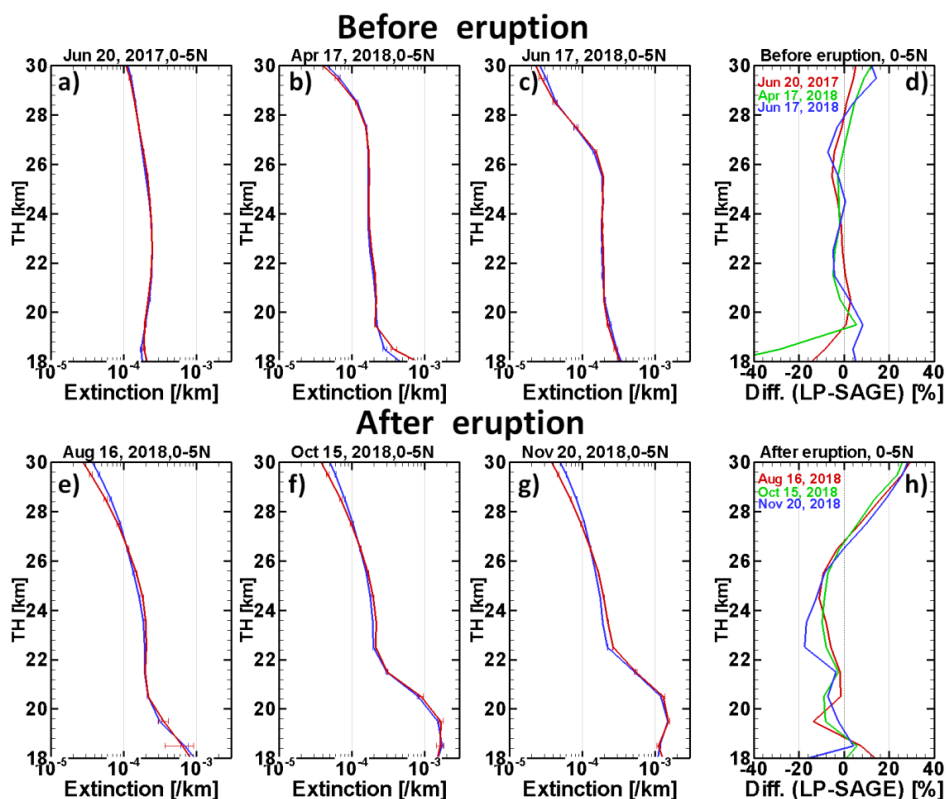
15

20

25



5

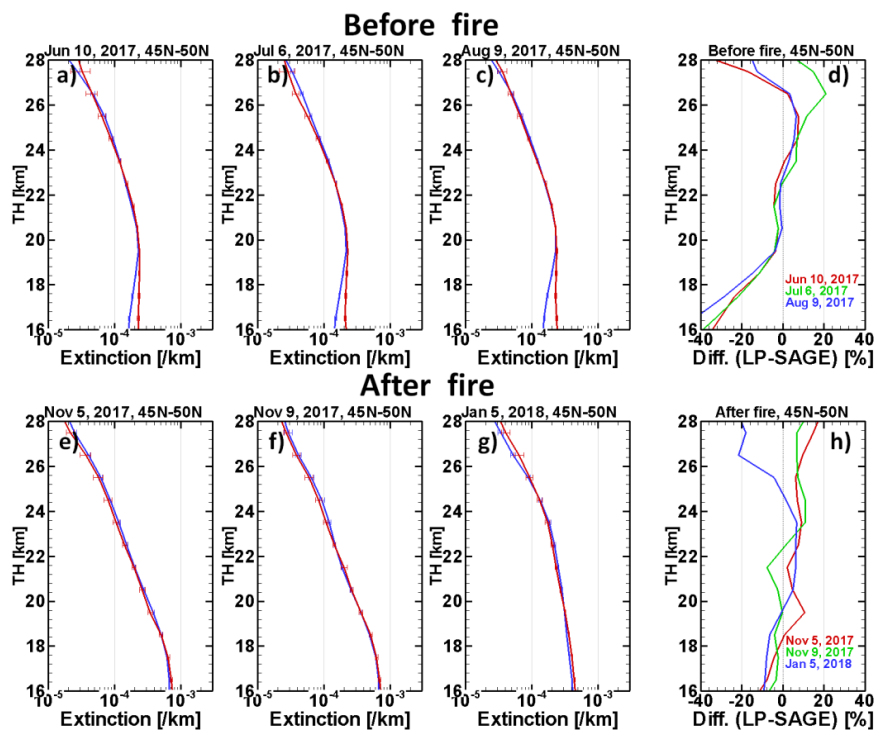


10 **Figure 6.** Comparison of daily zonal mean of OMPS/LP (blue) and SAGE III/ISS (red) aerosol extinction  
 profiles in latitude bin 0-5°N for six individual days prior to (a-c) and after (e-g) the Ambae eruption on  
 July 27, 2018. The corresponding relative differences between LP and SAGE are also shown in (g) and  
 (h). The horizontal error bars on the mean extinction profiles indicate standard error of the mean,  $\sigma/\sqrt{N}$ .  
 Enhanced extinctions around 20 km after the eruption (e-g) are observed compared to (a-c).

15



5



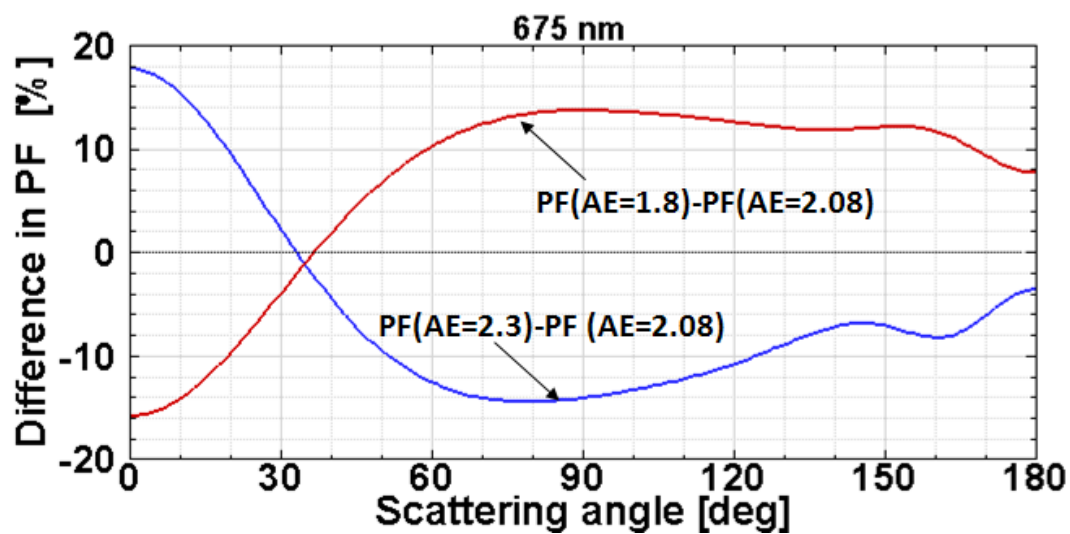
10 **Figure 7.** Comparison of daily zonal mean of OMPS/LP (blue) and SAGE III/ISS (red) aerosol extinction  
 profiles in latitude bin 45° N – 50° N for six individual days prior to (a–c) and after (e–g) the Canadian  
 PyroCb event in 2017–18. The corresponding relative differences between LP and SAGE are also shown  
 in (g) and (h). The horizontal error bars on the mean extinction profiles indicate standard error of the  
 mean,  $\sigma/\sqrt{N}$ . Enhanced extinctions around 20 km after the fire (e–g) are observed compared to (a–c).

15

20



5



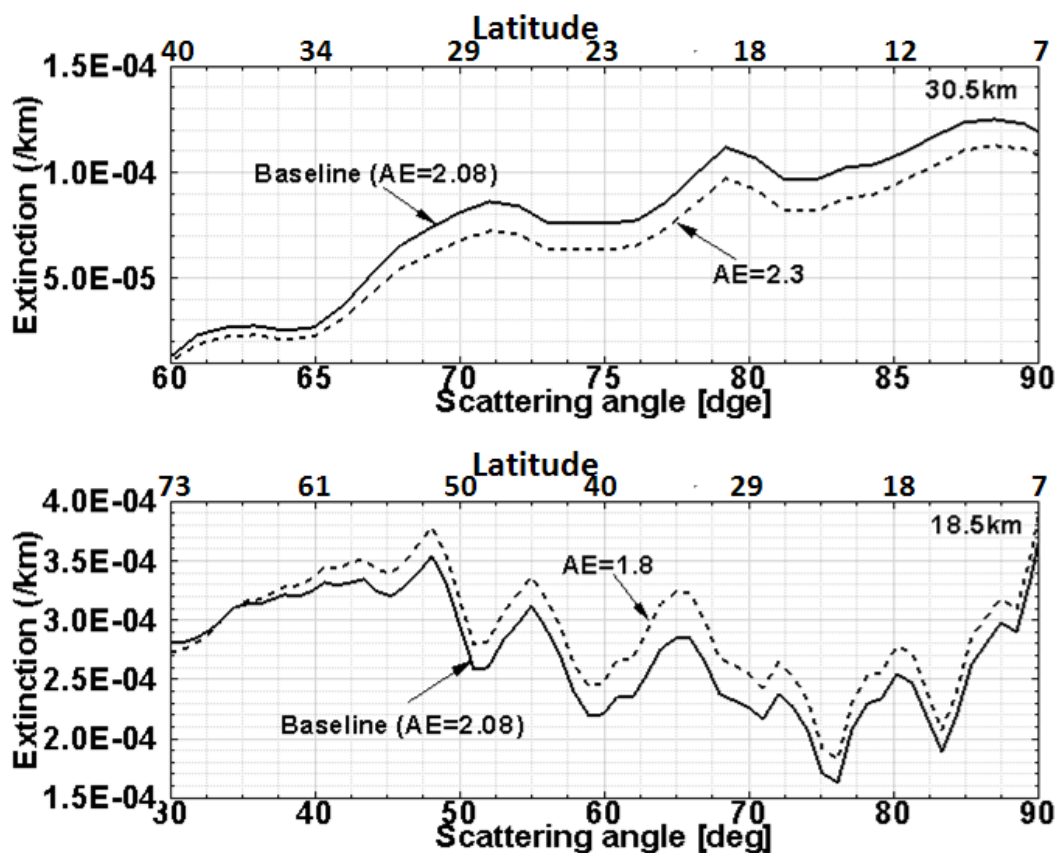
10 **Figure 8.** This figure shows how aerosol phase function (PF) at 675 nm changes when AE is perturbed by  $\pm 10\%$  of the baseline value of 2.08.

15

20



5

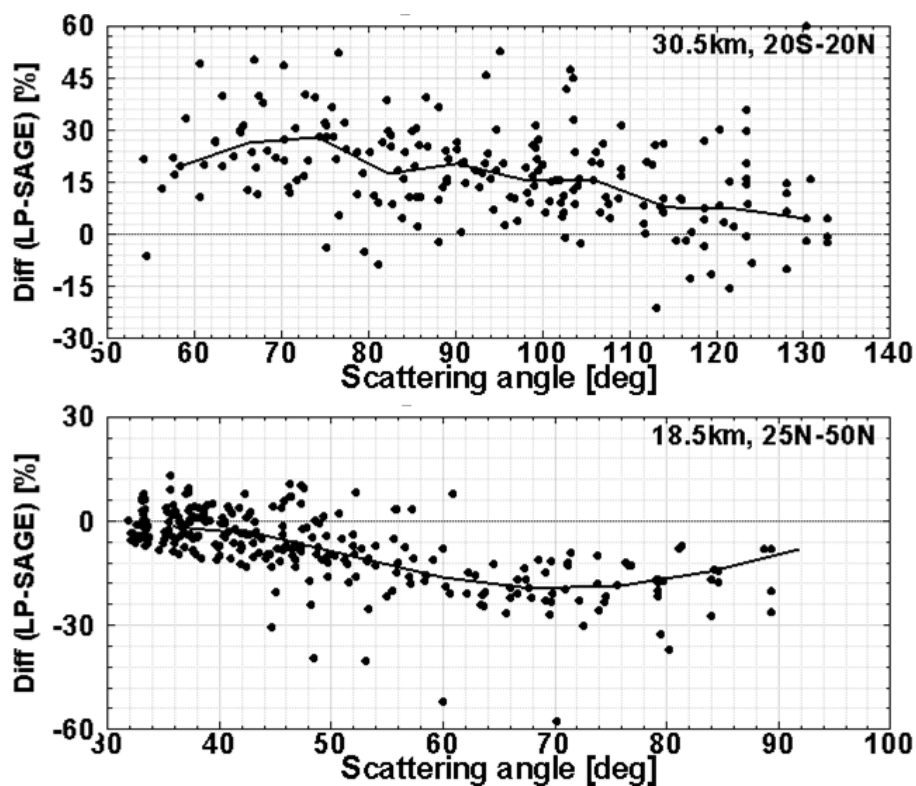


10 **Figure 9.** LP retrieved extinctions from baseline particle size distribution (solid line) and from the same with Angstrom Exponent (AE) adjusted by  $\pm 10\%$  (dashed line) for altitude at 30.5 km (top panel) and 18.5 km (bottom panel) as a function of scattering angle (x-axis bottom) and latitude (x-axis top) using OMPS/LP measurements for a single orbit on September 12, 2016. While extinctions at 30.5 km with AE=2.3 are lower than the baseline, extinctions at 18.5 km with AE=1.8 are higher than the baseline.

15



5



10 **Figure 10.** Relative differences in aerosol extinction between LP and SAGE III/ISS along with the median difference (solid line) as a function of LP scattering angle for altitude at 30.5 km in latitude bin 20° S - 20° N (top) and 18.5 km in latitude bin 25° N - 50° N (bottom) during the period of June 2017 - May 2019. The differences in aerosol extinctions vary significantly with scattering angle between 50–100 degree.

15





5

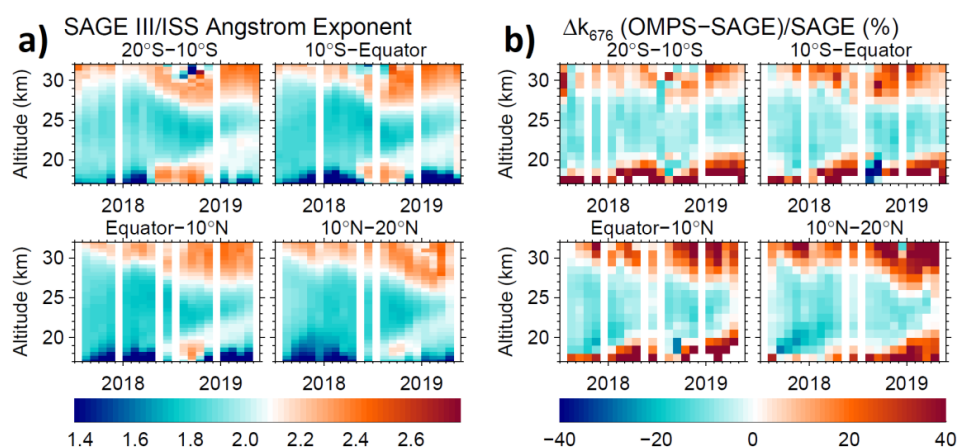


**Figure 11.** Monthly mean AE (a) and differences between SAGE III/ISS and OMPS/LP extinctions at 675 nm (b) in % as a function of altitude and time for four latitude bands in the tropics. The AE is derived from vertically smoothed SAGE III/ISS data using the aerosol extinctions at 520nm (interpolated) and 1020nm (reported) plotted on a color scale with the baseline value of 2.08 used for the OMPS-LP algorithm at its center.

15

20



5

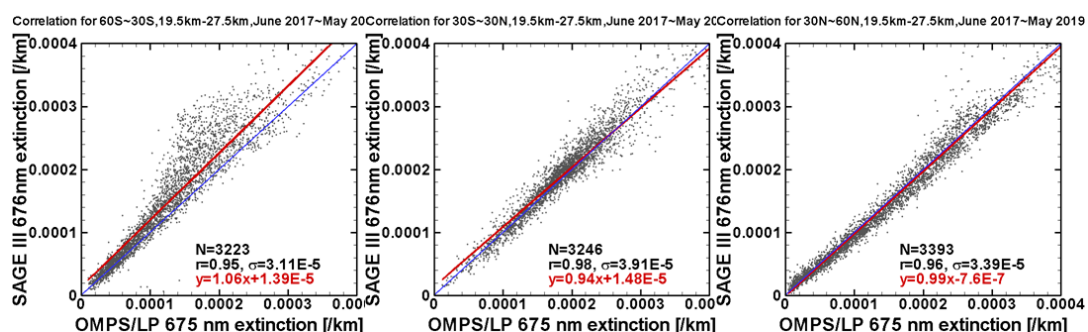


**Figure 12.** Scatter plot of SAGE III/ISS and OMPS/LP daily zonal means of extinctions between 19.5–27.5 km for 60°S - 30°S (left), 30°S - 30°N (middle), and 30°N - 60°N (right) for the entire time period of June 2017~ May 2019 illustrating the correlation between the two instruments. The red line show the linear regression between the data points, and the blue line represents a 1:1 relationship. The correlation coefficient  $r$ , the standard deviation of the differences ( $x-y$ )  $\sigma$ , and the number of elements  $N$  used to compute  $r$  are also shown.

15

20

25



5

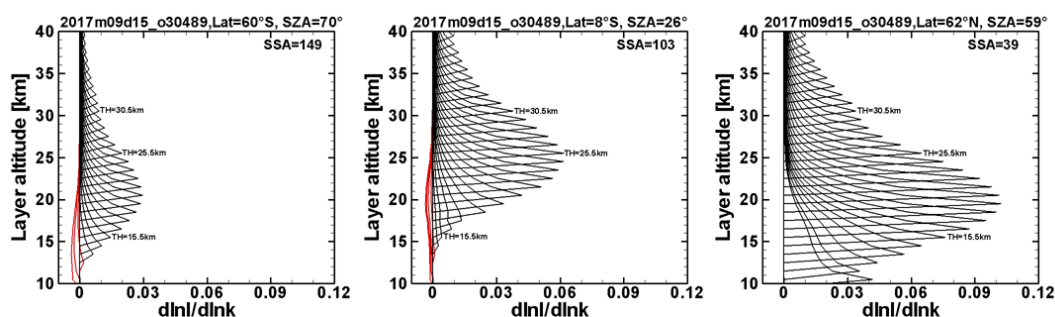


**Figure 13.** Example of aerosol weighting functions at wavelength 675 nm for altitude at 60° S (left), 8° S (middle) and 59° N (right). Each curve represents the sensitivity of the modelled LP radiance,  $I$ , at a given tangent altitude, TH, to a typical aerosol extinction  $k$  at each 1 km altitude layer from 10 to 40km. The weighting functions are positive (black line) and peaked at different altitude ranges. At lower TH altitudes and for larger SSA, the 675nm weighting functions become negative (red line) and loose sensitivity to aerosol extinction at lower TH altitudes.

15

20

25